CIMTEC 2002 - 3rd Forum on New Materials
4th International Conference
"Advanced Inorganic Structural Fiber Composites"
P. Vincenzini, C. Badini (Editors) © Techna Srl, 2003

HIGH TEMPERATURE PROPERTIES OF CVD-SiC AND CVD-DIAMOND MONOFILAMENTS

Georges CHOLLON, Roger NASLAIN

Laboratoire des Composites Thermostructuraux (LCTS), UMR 5801 (CNRS-SNECMA-CEA-UB1), Université Bordeaux 1, 3, allée de La Boétie, 33600, Pessac, France.

Robert SHATWELL, QinetiQ, Cody Technology Park, Farnborough, Hampshire, GU14 0LX, UK.

Paul MAY, School of Chemistry, University of Bristol, Cantock's Close, Bristol, BS8 1TS, UK.

The chemical, structural and thermomechanical properties of CVD-SiC and diamond filaments have been investigated. Electron and Raman microprobe analyses showed graded radial atomic and phase distributions in the SiC filaments. Thermo-mechanical investigations (tensile/bending elastic modulus/creep tests) were carried out on single filaments and these properties were correlated with the physicochemical features. The thermal behaviour of the CVD-SiC filaments is strongly related to the nature and the amounts of intergranular secondary phases (free carbon and silicon). The strong covalent bonds and the microcrystalline state of the CVD-diamond filaments give rise to an outstanding thermal behaviour.

1 INTRODUCTION

SiC based filaments are potential reinforcements for metal or ceramic matrix composites (MMC, CMC) because of their attractive properties such as high strength, stiffness and creep resistance. Two main companies provide CVD-SiC filaments: Textron Specialty Materials, Lowell, USA and the Defense Evaluation and Reseach Agency (DERA), Farnborough, UK.

The SCS-6 filament is a carbon core 140 µm filament produced by Textron. The CVD-SiC sheath is carbon rich near the carbon core while stoichiometric near the surface. It is subsequently covered by a 3 µm multilayer pyrocarbon coating [1].

The DERA has produced a 100 µm (SM1140+) and a 140 µm (SM1156) tungsten

core SiC based filaments. Both filaments are coated with a 5 μm pyrocarbon layer. The SM1140 CVD-SiC coating is stoichiometric near the tungsten core and silicon rich in the outer part [2-3]. New experimental filaments have been under development at DERA, aiming to improve their mechanical properties and thermal stability. A 140 μm near stoichiometric filament has been produced. This is referred to as SM1156*.

CVD-diamond filaments are other very interesting candidates as reinforcing constituents for MMC or CMC. They display outstanding Young's modulus values, close to that for bulk diamond [4-5]. Moreover, they are expected to show a very high creep resistance and maintain their stiffness up to high temperatures in inert conditions, as long as graphitization do not occur (T>1600°C in vacuum or argon). In the present case, the diamond coating was deposited on a 50 μm tungsten core [6], the outer diameter of the filaments ranging from 120 to 150 μm (i.e., 82-89 vol.% diamond).

This paper reports a systematic and comparative characterisation of SiC and diamond filaments in terms of elemental composition and microstructure, using the SCS-6 filament as reference. Various thermomechanical analyses have been made (Young's modulus, creep and relaxation at high temperature) and the results correlated with the chemical and phase content of the filaments.

2 MATERIALS

Four types of filament have been studied: SCS-6, from Textron, SM1156 and SM1156* from QinetiQ and a CVD-diamond filament from the University of Bristol. Their main feature are summarised in table 1.

	SCS-6	SM1156	SM1156*	CVD-diamond
$Ø_{ext}$(μm)	144	147	141	120-150
$Ø_{core}$(μm)	C(33+3)	W(15)	W(15)	W(50)
$e_{coating}$(μm)	Pyrocarbon(3)	Pyrocarbon(5)	Pyrocarbon(5)	-
$E_{tensile}$(GPa)	356±5	331±4	385±5	930±15[a]
$E_{bending}$(GPa)	385±10	310±8	354±10	1040±30[b]

Table 1: Main features and elastic modulus at room temperature of the filaments ([a] $Ø_{ext}$=123 μm, [b] $Ø_{ext}$=143 μm)

3 EXPERIMENTAL

Electron probe microanalyses (EPMA) (SX 100 from CAMECA, France) were conducted on polished cross-sections of filaments. Linescan measurements were performed along the radius of the filaments, with a spatial resolution of about 1 μm^3.

Raman microspectroscopy (RMS) analyses (LABRAM 010 from Dilor, France) were conducted on the same samples as those for EPMA. The excitation source was the 633 nm line of a He/Ne laser. Linescan measurements were recorded along the diameter of the fibers.

The diameter of the filaments was measured using laser interferometry.

Tensile tests were carried out at room temperature to measure the Young's modulus of the monofilaments. A direct strain measurement device was used (to avoid any compliance effect, derived from a commercial extensometer.

Three-point bending tests were performed with a thermomechanical analysis (TMA) testing device (TMA SETSYS 2400, Setaram) on single filaments, at high temperature in argon (10^5 Pa). These tests allowed both the measurements of the bending modulus and the flexural creep. The specimens were all loaded with a 12 mm span alumina device ($F<3.10^{-2}$ N).

Tensile creep measurements were performed at high temperature in argon (10^5Pa). The filaments were submitted to a stress of 0.3MPa.

Bend stress relaxation (BSR) tests were conducted on the filaments in argon (10^5Pa) for a time t=1 h. The thermal behaviour of the samples is characterised by the stress relaxation ratio $m=1-R_0/R$, where R_0 and R are respectively the initial curvature imposed to the filament and the final one (R_0=60 mm).

4 RESULTS AND DISCUSSION

4-1 Chemical and structural analyses

SM1156 filament

The SM1156 filament consists of stoichiometric SiC near the tungsten core only (Fig. 1a). The silicon concentration gradually increases outward to reach a free silicon excess of about 10 at.%.

The SiC-TO feature is particularly sharp near the tungsten core (795 cm^{-1}), indicating a high crystalline state (Fig. 2b). It broadens and weakens rapidly outwards, showing a strong decrease of the SiC grain size from micro to nanocrystallites. An additional broad band at 400-550 cm^{-1} appears while reaching the outer part, assigned to amorphous free silicon (as suggested by EPMA).

SM1156 filament*

The SM1156* filament shows a slight carbon excess (about 8 at.%) close to the tungsten core (Fig. 1b). The free carbon amount fluctuates slightly while decreasing from the core to about 20 µm. The composition remains almost stoichiometric throughout the rest of the deposit, but still with a carbon excess.

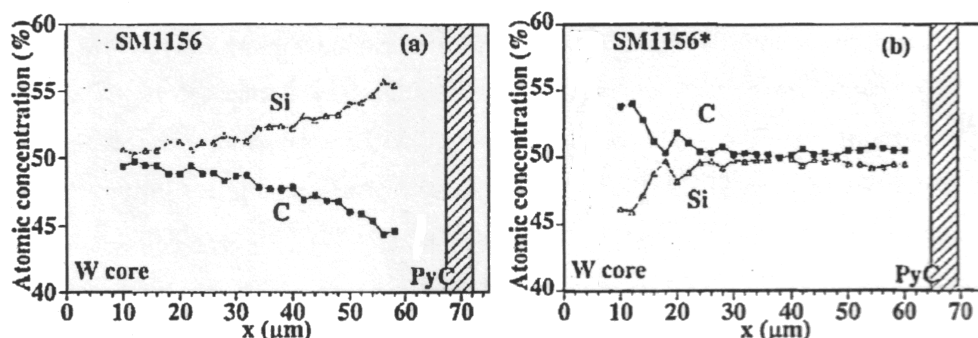

Fig. 1:EMPA radial profiles of the CVD-SiC filaments. (a) SM1156, (b) SM1156*.

The Raman carbon features are clearly visible as a single broad band at 1100-1700 cm^{-1}, characteristic of a very disordered form of carbon. The evolution of the intensity of this band along radius corroborates almost exactly the free carbon concentration obtained by EPMA. The SiC phase is rather well crystallised in the β form (3C polytype) (TO and LO modes at 795 and 970 cm^{-1} respectively) and no free silicon (400-550 cm^{-1}) is detected throughout the filament.

CVD-diamond filament

Whereas all the CVD-SiC filaments have smooth surfaces, the CVD-diamond deposit shows a rough microstructure with highly textured and columnar microcrystals (Fig. 3). The Raman spectra recorded along the cross section are rather similar. In addition to an intense photoluminescence background, the spectra clearly show the sharp diamond characteristic peak (TO=LO phonon) at about

1335cm^{-1} (Fig. 4). The peak position changes slightly, probably because of local stress variations [5].

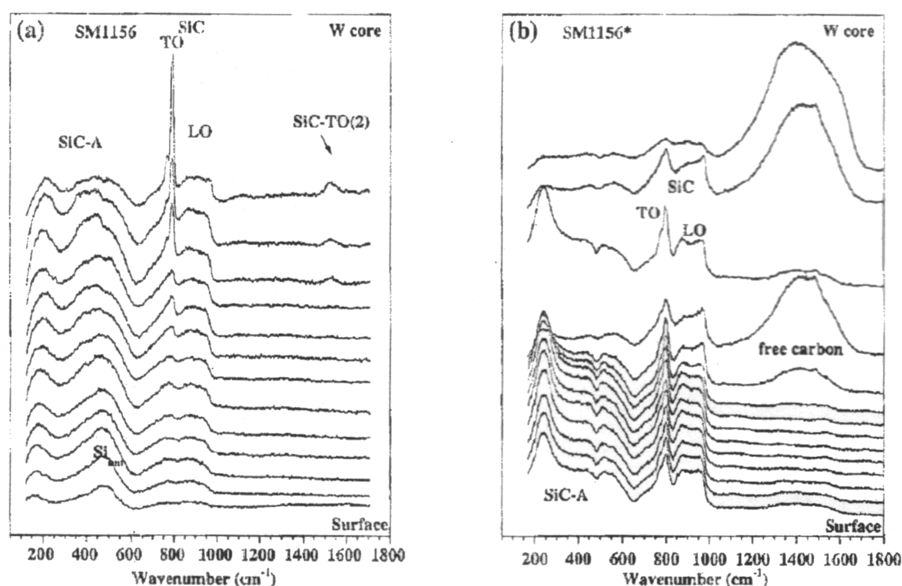

Fig. 2:RMS spectra of the CVD-SiC filaments. (a) SM1156, (b) SM1156*.

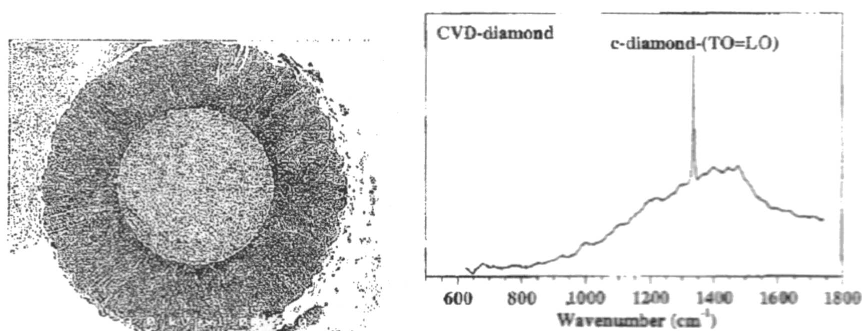

Fig. 3:CVD-diamond filament Fig. 4:RMS spectrum of the CVD-diamond

4-2 Thermo-mechanical analyses

Elastic modulus

The average Young's modulus as measured in tension of the various filaments ($E_{tensile}$) is shown in Table 1. Whereas the Young's modulus of the three CVD-SiC filaments currently ranges from 330 to 385 GPa, it is as high as 930 GPa for the CVD-diamond filament. Using the rule of mixture, the modulus of the sole CVD-diamond coating reaches 1030 GPa, close to the theoretical value for bulk diamond

(1.2 TPa) [4]. The SM1156 filament shows a modulus significantly lower than that of the near-stoichiometric SM1156* filament. Such a low value is unambiguously due to the rather high amounts of free silicon in the former (E_{si}=190 GPa, for an average silicon fraction of about 5 vol.%). The Young's modulus of the SCS-6 filament is in-between the two, the frée carbon phase of the inner region likely resulting in a decrease of stiffness.

The bending modulus ($E_{bending}$) of the various filaments is also reported in table 1. $E_{bending}$ is rather characteristic of the near-surface part of the filament, which is mostly stressed in bending. This is indeed the case for the 50 µm core CVD-diamond filament, where the modulus gets closer to the expected value. The contribution of the pyrocarbon coating is also thought to be responsible for the lower modulus in bending of both SM1156 and SM1156*. $E_{bending}$ may be also affected by the chemical and structural gradient along the CVD-SiC layer itself. The presence of a more compliant layer located either near the core (the free carbon rich layer in SCS-6) or near the surface (the free silicon rich layer in the SM1156), respectively results in a higher or lower value of $E_{bending}$ with respect to $E_{tensile}$.

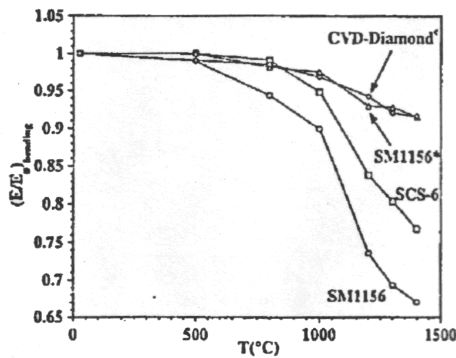

Fig. 5:Bending modulus versus test temperature [c] ($Ø_{ext}$=144 µm)

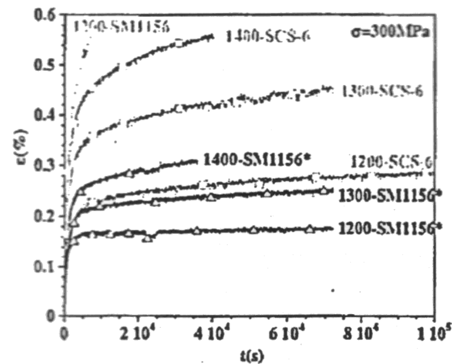

Fig. 6:Tensile creep behaviour of the filaments

The evolution of the bending modulus versus the test temperature is shown in Fig. 5. A decrease of $E_{bending}$ is observed with increasing T for all the filaments, but with drastically different amplitudes. The CVD-diamond and the nearly-stoichiometric CVD-SiC filaments show the best thermal stability. The CVD-diamond material has strong sp^3 covalent bonds and a large grain size. Therefore, it might be expected to show only a very limited decrease of $E_{bending}$ with temperature.

The slight drop observed may be assigned essentially to the contribution of the 50 μm tungsten core and minor superficial graphitisation (as observed by RMS) occurring at high temperature. The SM1156* filament shows the best thermal behaviour of all the CVD-SiC specimens. This is not only due to its nearly stoichiometric composition but also, to the existence of the free carbon phase. Free carbon as intergranular phase, is expected to show better thermal stability than free silicon (T_f(Si)=1410°C). The detrimental effect of intergranular free silicon to the elastic modulus is clearly noticeable for the SCS-6 filament [6], in which the slightly silicon-rich CVD-SiC layer is located at the highly stressed outer part. The same phenomenon is particularly apparent for the SM1156 filament, with higher amounts of free silicon near the surface.

Tensile creep

The tensile creep curves are presented in figure 6. Except for the SM1156 filament, which failed prematurely for T≥1200°C, all the tests were interrupted before rupture. The early failure of the SM1156 filament is due to the severe degradation of the W/SiC interface at high temperature. All the filaments mainly show only primary creep throughout the tests and over the entire temperature range. The correlation between the creep behaviour and the composition/microstructure of the filaments is particularly obvious. The SM1156* filament displays the best creep resistance of the three (approximately half of the creep strain of SCS-6), whereas SM1156 shows the worst (more than twice the SCS-6 strain). The creep behaviour of the SCS-6 filament has been extensively studied [7-8]. The creep rate controlling mechanism is generally admitted to be grain boundary diffusion (Coble creep). The creep behaviour is therefore significantly influenced by the nature of the grain boundary and the presence of an intergranular phase. The SM1156* filament, containing intergranular free carbon all along the CVD layer, therefore exhibits the best creep resistance, whereas the SM1156 filament, having large amounts of free silicon, shows the poorest. A variable load sharing is expected, as all the filaments actually consist of a multilayered composite material. This is particularly true for the SCS-6 filament, with load sharing between the inner carbon-rich layer and the outer nearly-stoichiometric sheath. This effect, together

with the microstructural changes occurring during creep, are likely to be responsible for the pronounced primary creep behaviour [7-8].

Bending creep

The bending creep curves are shown in figures 7a-b. Short unloading cycles (30 MPa) were carried out during the creep tests to prevent friction forces and to investigate the residual strain and the bending modulus, indicating a damaged monofilament. The CVD-SiC filaments show only primary creep at 1200°C. As in the tensile creep tests, the SM1156* filament shows the best creep resistance. The creep strain of the SCS-6 filament is about twice that of SM1156*, whereas the SM1156 strain is about fifteen times that of SM1156*. The discrepancy between the various CVD-SiC filaments is even more pronounced at 1400°C. Such different thermal behaviours can be explained by the different composition/microstructure of the filaments. As the near surface region is more loaded than the core, the creep bending behaviour reveals features of the outer CVD layers of the filaments. Whereas the SM1156* filament is rather homogeneous (except very near the W/SiC interface), the SCS-6 and SM1156 filaments both show a significant multilayered composite character, with both outer layers containing free silicon. The differences between the creep behaviour of the various CVD-SiC filaments is therefore more pronounced than for the tensile tests, particularly at high temperatures (T_f(Si)=1410°C).

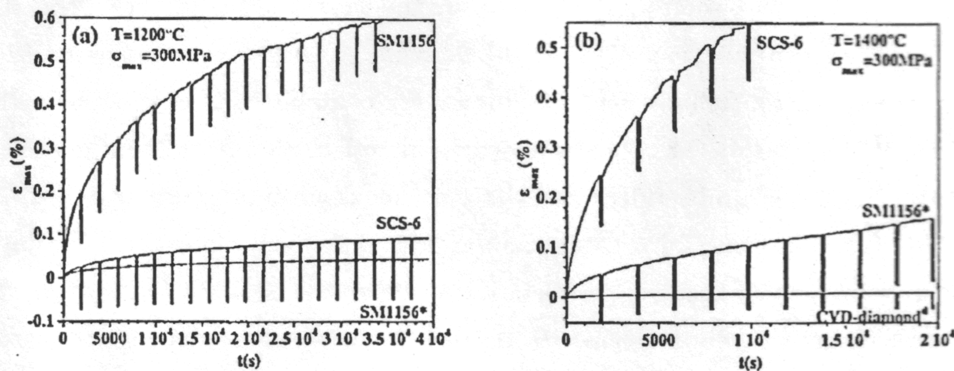

Fig. 7:Bending creep behaviour of the various filaments (^{d} $Ø_{ext}$=143 μm)

The CVD-diamond filament exhibits a considerably higher creep resistance than the CVD-SiC filaments. Despite the large 50 μm W core, the creep strain is only

about 1/13 that of the SM1156* filament. Besides the creep strain, the unloading cycles evidenced a slight and constant decrease of the bending modulus versus time. This phenomenon might be related to the superficial degradation of the CVD-diamond at high temperature, as shown by RMS.

Bend stress relaxation

The thermal evolution of the parameter m is presented in figure 8. A larger curvature (R_0=150 mm) had to be applied to the CVD-diamond filament owing to its lower fracture strain. For comparison, the same conditions were also used for the CVD-SiC filaments. The BSR resistance of the various filaments is consistent with the tensile and the bending creep behaviours. The BSR resistance of the SM1156 filament is significantly lower than that of the SCS-6 (about 250°C lower for given a m value), while they show similar thermal activation [7]. The SM1156* filament shows a BSR resistance improvement of about 150°C with respect to the SCS-6, but a lower thermal activation. Just as for creep, the lower BSR resistance of the SM1156 filament is related to the much larger excess of free silicon and the smaller SiC grain size of the outer layer. The better thermal resistance of the SM1156* filament is assigned to the presence of co-deposited free carbon. The CVD-diamond filament displays the best thermal stability of all the tested filaments, i.e., at least 250°C higher than SM1156*. The strong C-C covalent bond, the large grain size and the absence of low melting temperature and/or compliant intergranular phase, are responsible for the exceptional thermal behaviour of this filament.

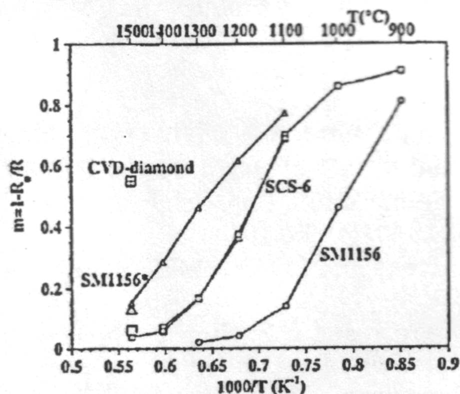

Fig. 8:BSR behaviour of the various filaments (large symbols:R_0=15cm)

5 CONCLUSION

The SCS-6 filament consists of a free carbon-rich inner layer and a near stoichiometric outer layer, with a slight silicon excess. The SM1156 filament composition is stoichiometric near the tungsten core and turns to a large silicon excess (10 at.%) near the surface. The SM1156* monofilament is carbon-rich near the core and near stoichiometric with a slight amounts of free carbon all along the CVD-SiC sheath. All these filaments contain a sub-micron SiC crystals, with decreasing grain size when increasing amounts of secondary phases. The CVD-diamond filament shows an homogeneous microcrystalline structure.

The thermomechanical behaviour of the CVD-SiC filaments (tensile or bending modulus and creep) depends on their radial composition and microstructure. The room temperature stiffness increases with decreasing amounts of compliant secondary phases (free carbon and silicon). The presence of intergranular free carbon results in a stable high temperature elastic modulus and an improved creep resistance. By contrast, free silicon leads to a catastrophic drop of high temperature stiffness and creep resistance. The tensile/bending creep tests have shown load bearing effects due to the composite multilayered composite structure of the CVD-SiC filaments. The CVD-diamond filament displays exceptional stiffness and creep behaviour up to high temperatures because the strong C-C covalent bonds, the large grain size and the absence of low melting temperature and/or compliant intergranular phase. If the growth rate and the failure strain can be increased to a reasonable levels, such filaments may find uses as CMM or CMC reinforcements.

REFERENCES

1) X.J. Ning and P. Pirouz, J. Mater. Res. **6** [10] (1991) 2234.
2) Y. Ward, R.J. Young and R.A. Shatwell, J. Mater. Sci. **36** (2001) 55.
3) G. Chollon and R. Naslain, Ceram. Eng. Sci. Proc. **21** [4] (2000) 339.
4) P.W. May, Endeavour **19** [3] (1995) 101.
5) E.D. Nicholson, J.R. Weeks and M.N.R. Ashford, Diamond and Related Materials **6** (1997) 817.
6) R.C. Warren, C.D. Weaver and S.S. Sternstein, Proc. of ICCM-11, vol. 4, M.L. Scott ed., Woodhead Publishing Ltd., (1997) 633.
7) G.N. Morsher, C.A. Lewinson, C.E. Bakis and R.E. Tressler, J. Am. Ceram. Soc. **78** [12] (1995) 3244.
8) C.A. Lewinson, L.A. Giannuzzi, C.E. Bakis and R.E. Tressler, J. Am. Ceram. Soc. **82** [2] (1999) 407.